

Bone Formation within Porous Hydroxylapatite Implants in Human Periodontal Defects

E. B. Kenney,* V. Lekovic,† J. C. Sa Ferreira,* T. Han,*
B. Dimitrijevic‡ and F. A. Carranza, Jr.*

Accepted for publication 2 May 1985

TISSUE SAMPLES FROM THREE SUBJECTS who had periodontal defects treated with a porous hydroxylapatite implant were investigated using light microscopy and scanning electron microscopy. The 3-month specimen showed connective tissue infiltration through the pores and a narrow zone of bone formation present along the walls of the pores. At 4 months, continued evidence of bone deposition was present with osteocytes, osteoblasts and organization of collagen fibers apparent throughout the implant. The 6-month implant had further evidence of continued bone formation with lamellar bone being the major component within the pores.

A process for preparation of artificial porous prosthetic materials from the skeletal structure of marine invertebrates was first reported in 1972 with replicates of methacrylate, tin, titanium oxide, chrome cobalt molybdenum and aluminum oxide.¹ This led to the development of Interpore 200,‡ a porous hydroxylapatite replicate based on the structure of common reef-building coral *Porites*.² After the organic components of the coral have been removed, the aragonite of the coral skeleton is converted to hydroxylapatite by treatment with an ammonium phosphate at elevated temperature and pressure. The hydroxylapatite is formed as small crystals³ in contrast to the large fused crystals found in the sintered or ceramic-like forms of artificial hydroxylapatite.⁴

The porous structure of Interpore 200 involves interconnecting pores of approximately 190 to 230 μm in diameter. When used as an implant, this porous structure allows ingrowth of connective tissue and vascular elements, which leads to ossification, with woven bone being first laid down and then later lamellar bone is present.^{5,6}

Numerous studies using Interpore 200 in a variety of animal model systems have all given consistent findings of bone growth into the pores when the material is implanted into bone. Finn et al.,⁷ using Interpore 200 as a mandibular interposition implant in dogs, found

complete connective tissue infiltration within the pores at 2 weeks. By 3 months the pores were partially filled with woven bone and osteoid. This was replaced at later time intervals by lamellar bone. Piecuch et al.,⁸ in a similar study, confirmed these results with lamellar bone and osteons seen at 12 months. Roser et al.⁹ provided further evidence for bone growth using mandibular onlays and inlays of Interpore 200 in dogs. When Interpore 200 has been used to fill defects created in bone in orthopedic studies, the pattern has been essentially the same as outlined above. Radial defects in dogs had 80% of the pore space filled with compact bone at 6 months and some biodegradation of the implant was seen.¹⁰ Other studies¹¹⁻¹⁴ on the use of Interpore 200 in long bone and mandibular defects in dogs and rats all have given the same evidence of bone growth into Interpore 200.

West and Brustein¹⁵ created chronic intraosseous periodontal defects in dogs and used Interpore 200 as an implant to fill these defects. At 6 months Interpore 200 was completely infiltrated with connective tissue and bone. A clinical study¹⁶ using Interpore 200 in human interproximal vertical defects demonstrated significant pocket reductions, attachment level gains and radiographic evidence of defect obliteration. However, at present there are no reports on the tissue dynamics when Interpore 200 is used to treat human periodontal defects.

MATERIALS AND METHODS

In the course of treating over 150 defects in human subjects, three samples of Interpore 200 have become

* University of California Los Angeles, School of Dentistry, Clinical Research Center for Periodontal Disease.

† University of Belgrade, Yugoslavia.

‡ Trademark of Interpore International, 18005 Skypark Circle, Irvine, CA.

available for histologic evaluation. In one subject (Case 1), Interpore 200 was placed on the labial surface of a lower incisor that had lost all of the labial bone due to periodontal destruction. This tooth had a hopeless prognosis and was extracted 3 months later. At the time of extraction, some of the labial gingiva containing the implant was removed and subjected to histological evaluation. In two other cases where interproximal defects were treated with Interpore 200 in a manner described previously,¹⁶ the implant became exposed at 4 months and 6 months (Cases 2 and 3), respectively. This exposure was related to extensive plaque formation and overfilling of the osseous defect. In these two cases the Interpore 200 implant was surgically removed and subjected to evaluation. The 6-month material was large enough to be divided in half so that one half could be viewed with light microscopy and the other half with scanning electron microscopy (Figs. 1-3).

All tissue samples were fixed in 3% glutaraldehyde



Figure 3. Case 3, 6 months after placement of Interpore 200. The coronal portion of the implant is visible in the interproximal region between the first molar and second premolar (arrow).

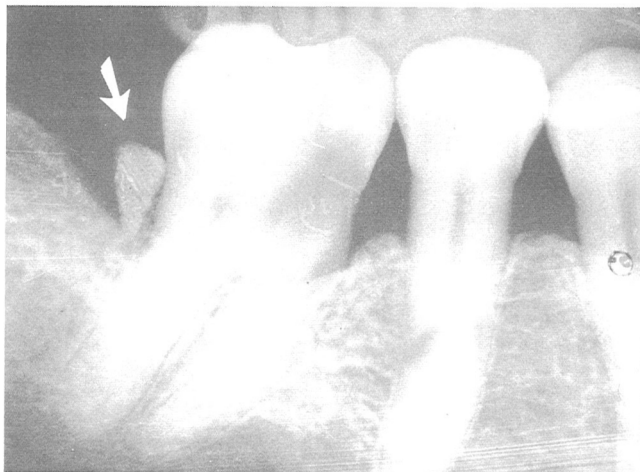


Figure 1. Radiograph of Case 2 at time of placement of Interpore 200 implant. The implant overfills coronal portion of the defect.

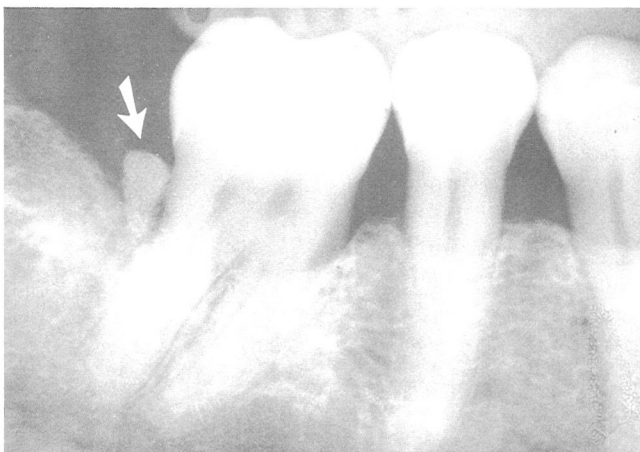


Figure 2. Radiograph of Case 2 at 4 months postoperative. The coronal portion of the implant has been trimmed after initial healing but there was exposure of the implant due to overfilling of the defect. Note radiographic changes in the apical portion of the implant consistent with osseous infiltration.

in Sorensen's phosphate buffer at pH 7.4. Material from Case 1 and Case 3 was decalcified with EDTA, embedded in paraffin and prepared for routine histological evaluation with 6- μ m sections and hematoxylin and eosin staining. Unstained histological sections were also evaluated under scanning electron microscopy after postfixing for 4 hours in 2% osmium tetroxide and drying according to the critical point method of Anderson.¹⁷ A coating of palladium and gold was then applied and the specimens were examined in a scanning electron microscope operating at 10 to 20 mV with various tilting angles.

The solid samples from Cases 2 and 3 were prepared for scanning electron microscopy as outlined above without decalcification, and the surface configuration was explored. Following this the samples were split open, recoated with metal and the internal surfaces evaluated with scanning electron microscopy.

This study therefore had samples of Interpore 200 at 3 months, 4 months and 6 months. The 3-month sample was decalcified and processed for light microscopy, and sections were viewed with the light microscope and the scanning electron microscope. The 4-month sample was undecalcified and viewed with scanning electron microscopy. The 6-month sample was divided in half. One half was decalcified and processed for light microscopy, the other half was not decalcified and used for scanning electron microscopy.

RESULTS

The 3-month sample (Case 1) was different from the other samples in that the implant had been placed coronal to the alveolar crest and not into a vertical defect. Light microscopy showed no evidence of inflammation associated with the implant. The pores of the implant were all filled with connective tissue and vascular elements. At the border of the connective tissue lining the pores of the Interpore 200, an eosinophilic

band approximately 5 to 15 μm wide was always present. This band had the appearance of early bone formation (Figs. 4 and 5). In order to discern the structure of this band, the tissue-sections were studied under scanning electron microscopy. This technic revealed collagen fibers in the central area of the pores with the periphery containing an apparently calcified collagenous tissue with all the features of early lamellar bone. No evidence of osteoclasts was seen in any of the sections (Figs. 6–8).

Under scanning electron microscopy the surface of the 4-month specimen (Case 2) showed complete coverage with collagen fibers and cells resembling fibroblasts (Figs. 9 and 10). The crystalline structure of Interpore 200 was not visible on the surface. The clusters of crystals typical of Interpore 200 were seen in some areas of the split surface, but in other areas this structure was covered with connective tissue (Fig. 11). The internal split surfaces showed infiltration of all pores with connective tissue in the apical two thirds of the specimen. The coronal one-third had some areas where bacterial invasion of the connective tissue within the pores had occurred. In the apical two-thirds there

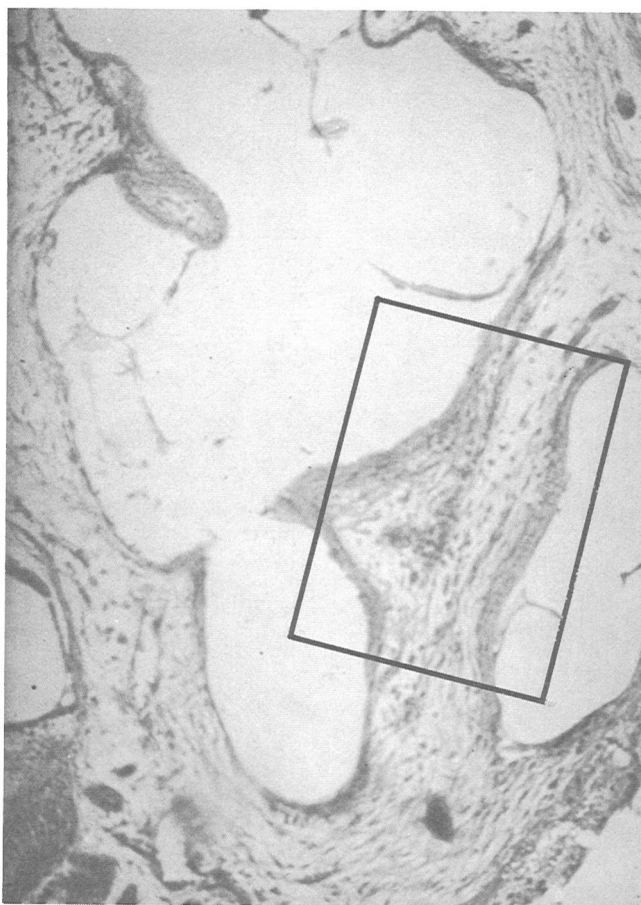


Figure 4. Photomicrograph of decalcified tissue section of gingiva with Interpore 200 implanted for 3 months (Case 1). Connective tissue and vascular elements have invaded the pores. The Interpore 200 has been removed from the section during decalcification leaving the voids (magnification $\times 180$).

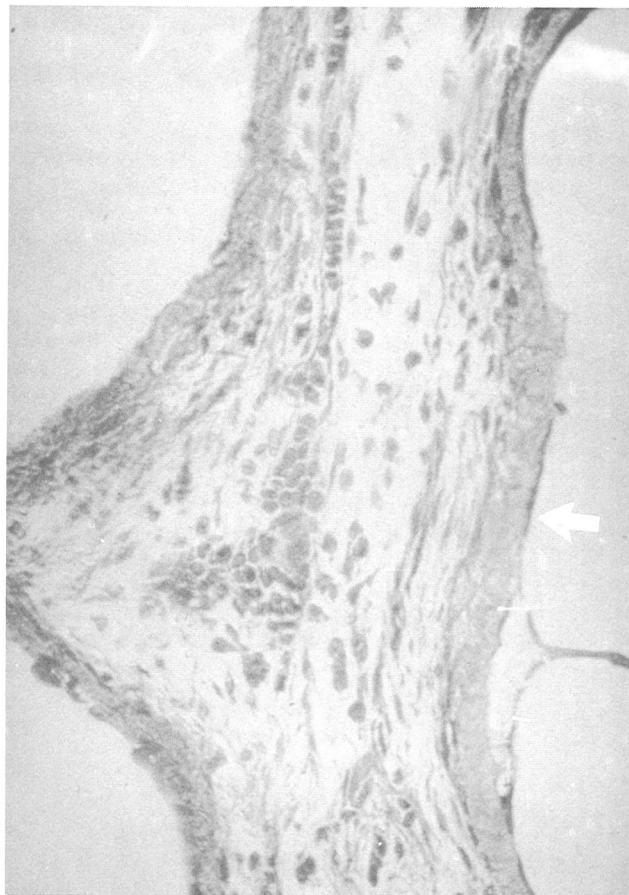


Figure 5. High power view of area in rectangle of Figure 4. Note the vascularity and absence of inflammation in the connective tissue within the pores. At the boundary between the pores and the implant, there is a layer of immature bone (arrow) (magnification $\times 465$).

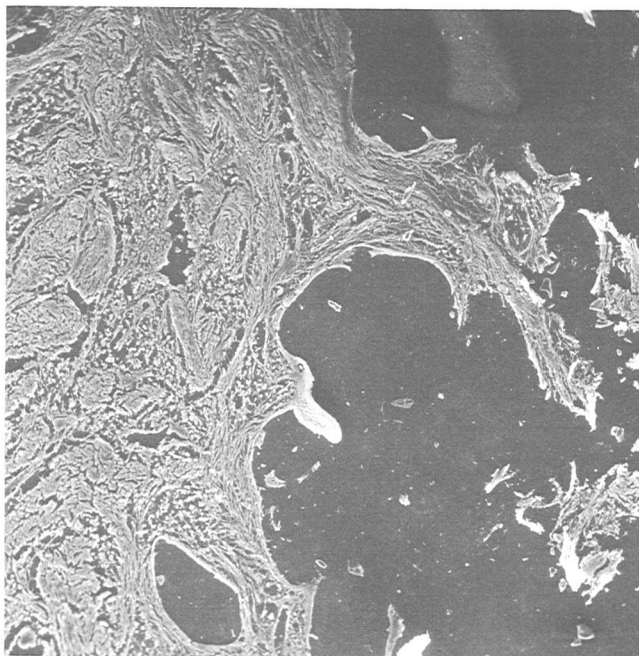


Figure 6. Scanning electron micrograph of tissue section from Figure 4 (magnification $\times 80$).

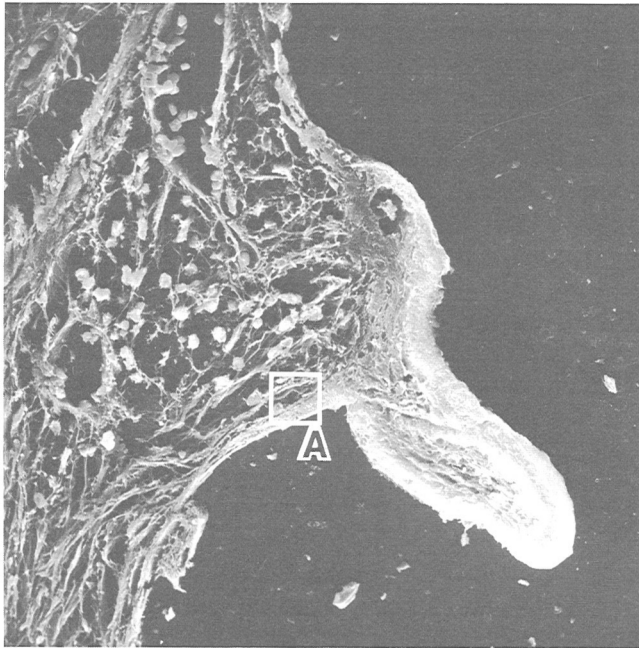


Figure 7. Magnification of central area in Figure 6 showing connective tissue fibers and blood vessels in the interpore space. The formation of new bone can be seen along the periphery of the pore (magnification $\times 400$).

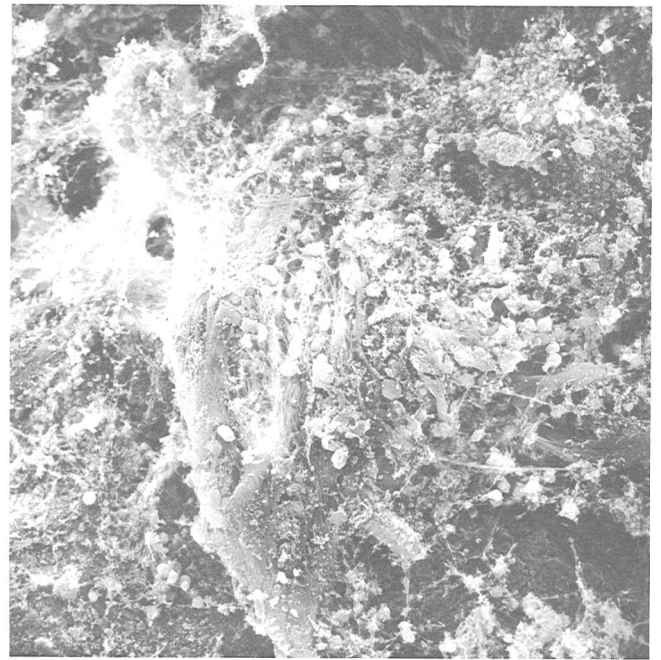


Figure 9. Scanning electron micrograph of surface of Interpore 200 implant at 4 months (Case 2). There are collagen fibers in large and small bundles completely covering the surface (magnification $\times 800$).

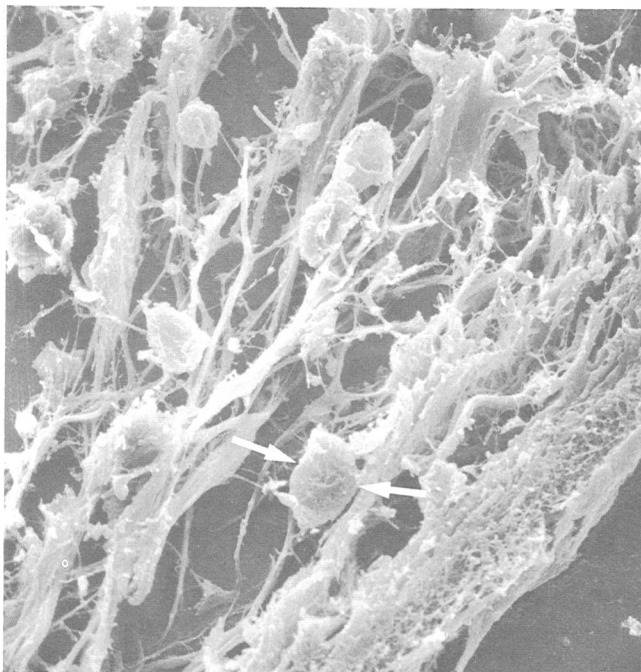


Figure 8. Magnification of rectangle A in Figure 7. Collagen fibers of the ingrowing tissue are blending with the early bone formation occurring along the lining of the pore. Connective tissue cells are seen adjacent to the newly formed bone (arrows) (magnification $\times 1600$).

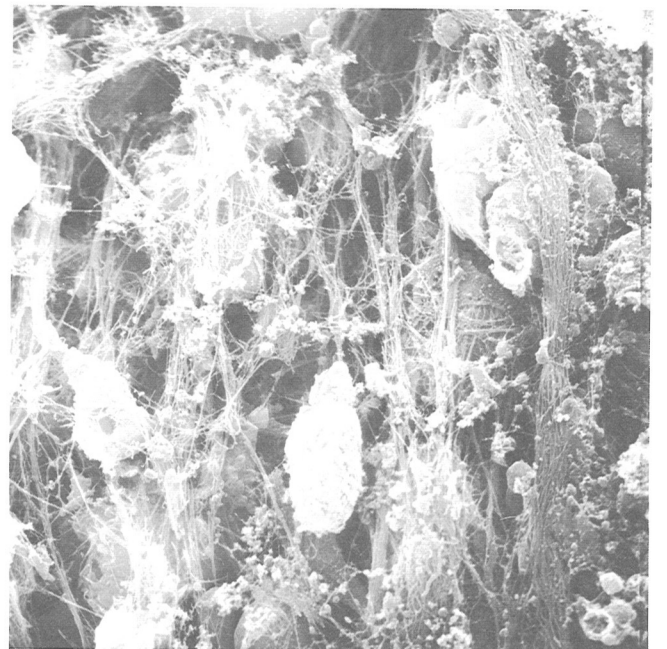


Figure 10. Scanning electron micrograph of central area of Figure 9. Individual collagen fibers are visible together with fibroblasts (magnification $\times 2000$).

was evidence of calcification of collagen fibers, and osteocytes were seen in calcified lacunae with structures identical to those previously reported as matrix vesicles¹⁸ on the surface of these cells and adjacent collagen fibers (Figs. 11 and 12). In one area, collagen fibers were seen emerging from a calcified matrix in a

pattern identical to that present in calcifying bone. In two areas, cells with the appearance of osteoclasts were present.

The scanning electron micrographs from the 6-month specimen (Case 3) showed that the surface of the implant had a similar appearance to that seen at 4 months. The internal surface had a few bacteria present within the pores in the superficial portion, but the

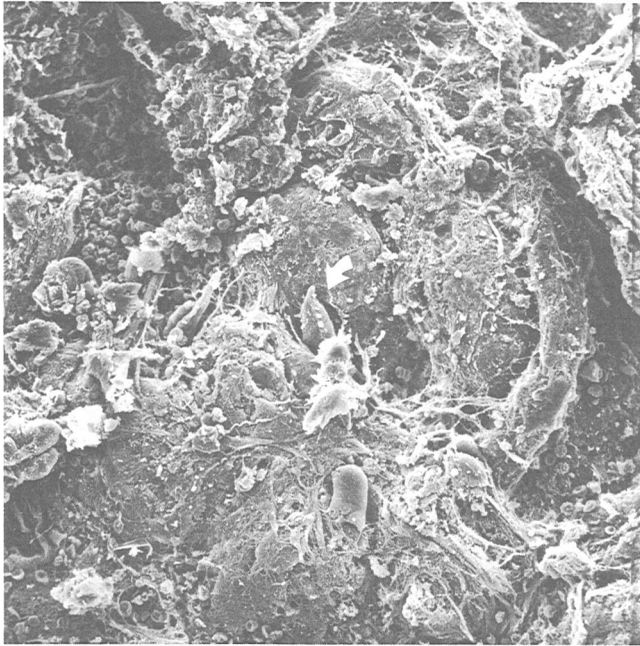


Figure 11. View of split surface of implant from Case 2 under scanning electron microscopy. The fracture of the implant has exposed an area where the typical crystalline structure of Interpore 200 is visible in the upper left corner. In the center of the field an osteocyte is seen in a typical osseous lacuna (arrow) (magnification $\times 400$).

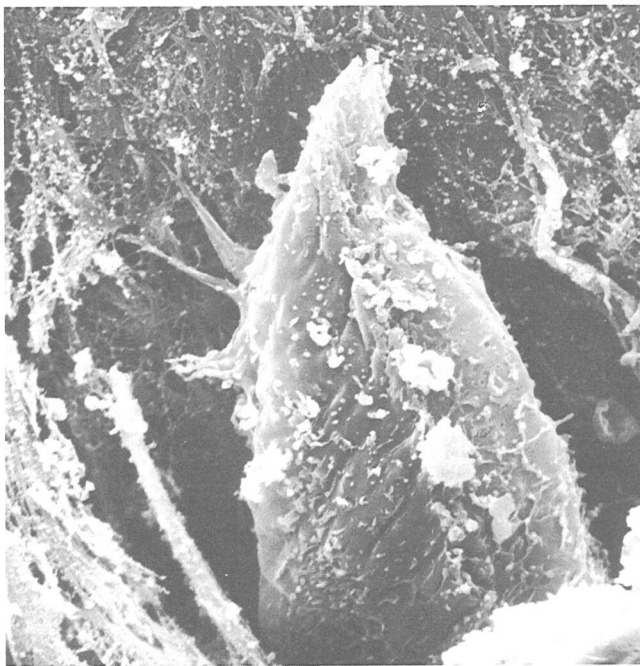


Figure 12. Magnified view of central portion of Figure 11. The cell present is an osteocyte with cell extensions running into the adjacent solidified collagen. Individual collagen fibers are also present. On the surface of the cell there are small particles similar in appearance to matrix vesicles (magnification $\times 4000$).

majority of the implant was full of connective tissue (Figs. 13–15). In many areas sheets of osteoblasts were present (Figs. 16 and 17). The implant appeared to have all of its external and internal surfaces covered with connective tissue. Cells typical of osteocytes sitting in lacunae were seen on the split internal surface of the

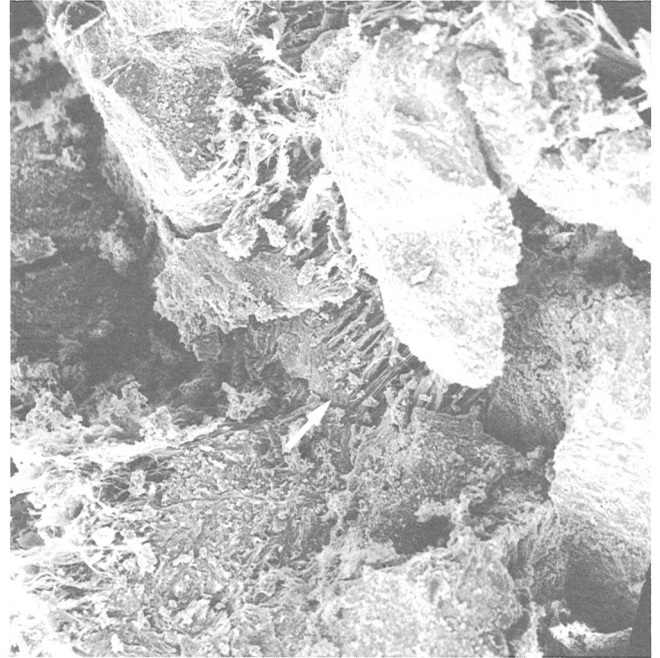


Figure 13. Split surface of implant from Case 3 (6 months). The internal walls of the pores are covered with bone and evidence of the central core of collagen is seen (magnification $\times 400$).

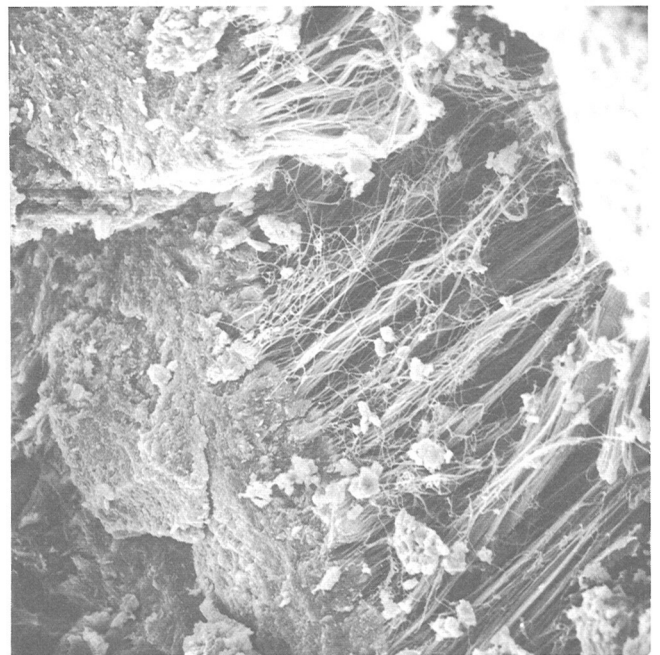


Figure 14. Magnification of central portion of Figure 13. Collagen fibers arranged in a parallel fashion are seen entering calcified bone (magnification $\times 2000$).

implant. The collagen fibers appeared to be more organized than in earlier samples and areas were seen within the pores where parallel groups of fibers were running into a calcified portion of tissue (Figs. 14 and 15). The light microscopic picture confirmed these findings with seams of lamellar bone lining all the pores. These seams varied in width and in some areas almost completely filled the pore space (Figs. 18 and 19). The central core space was occupied with connective tissue

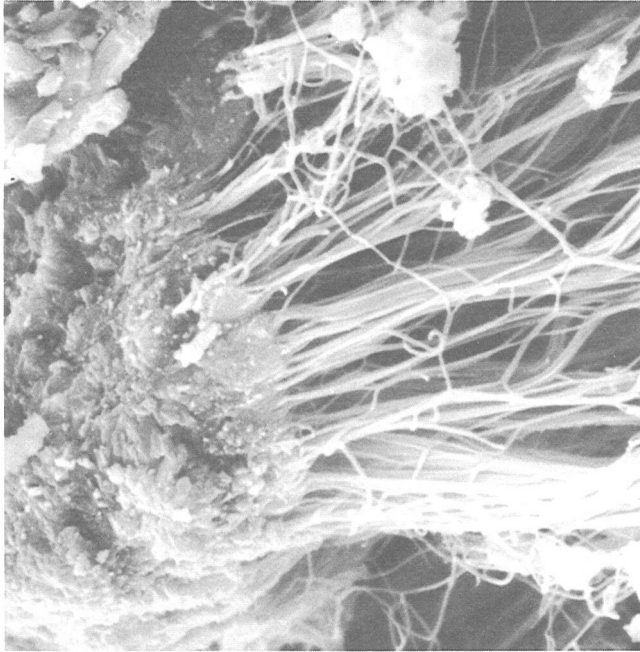


Figure 15. Magnification of upper right portion of Figure 14. Individual collagen fibers are present with their terminal ends being confluent with bone (magnification $\times 8000$).

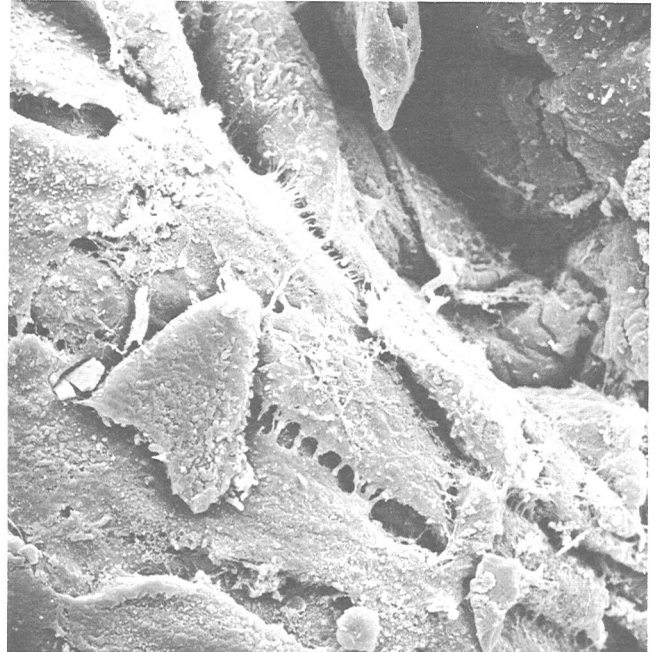


Figure 17. Magnification of lower central portion of Figure 16. Individual osteoblasts are clearly visible forming a syncytium (magnification $\times 2000$).

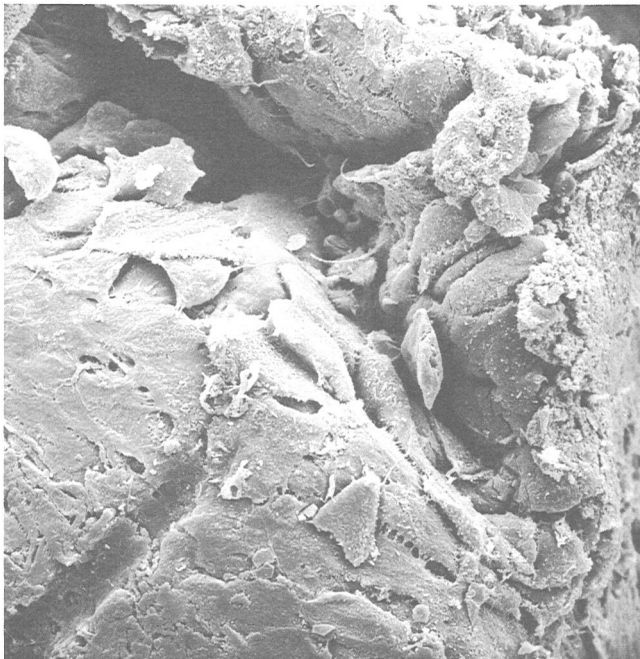


Figure 16. Another area of the split implant from Case 3. Sheets of osteoblasts are present covering the visible internal portion of the pores. Intercell connections are visible (magnification $\times 800$).

and in some isolated areas there was infiltration with inflammatory cells, primarily polymorphonuclear leukocytes.

DISCUSSION

The findings of this study provide evidence that Interpore 200 has the ability to facilitate osteogenesis within the porous structure of the implant when placed in human periodontal defects. This is in contrast to

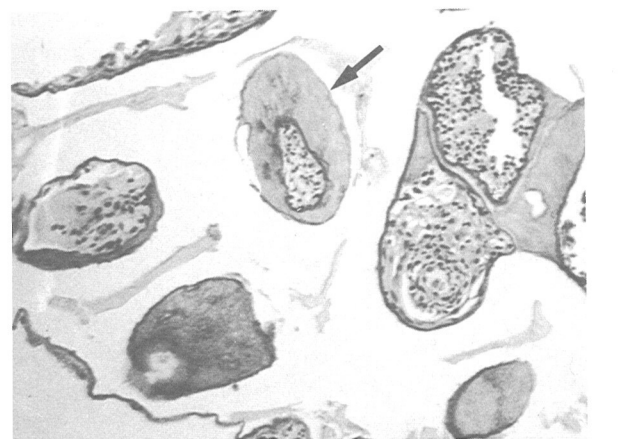


Figure 18. Photomicrograph of implant at 6 months after decalcification and histologic sectioning (Case 3). The spaces are areas previously occupied by implant. The pores are seen to be filled with a central core of connective tissue with a wide peripheral band of lamellar like bone (magnification $\times 36$).

histological reports of other hydroxylapatite implants which have to date failed to stimulate bone formation in human subjects.¹⁹⁻²¹

It appears that the process of connective tissue infiltration followed by the production of bone is similar in the human periodontal environment to that previously reported in animal model systems.⁷⁻¹¹ Apparently, this process occurs at a slower rate in human periodontal tissues than that seen in dogs and rats. Unfortunately, at present there are no human block sections available to substantiate the changes that occur in the periodontal ligament or cementum of teeth treated with Interpore 200. Therefore, it is not possible to know if regeneration of a normal periodontium occurs, even though clinical



Figure 19. High power view of Figure 18 with osteocytes seen within the lamellar bone (magnification $\times 120$).

trials suggest that new attachment is a part of the postsurgical healing following implantation of Interpore 200.¹⁶

The scanning electron micrographs showed within the implant cells similar to those reported as osteoblasts in cell culture and in the growing long bones of rats.^{18,22} This would be expected on the basis of the osteogenesis seen in all the specimens evaluated in the present study.

In several areas the scanning electron micrographs revealed rounded fibroblasts mixed with collagen fibers. No flattened or elongated forms were seen. Previous reports have shown that fibroblasts can have a variety of shapes with rounded forms commonly being present.²³⁻²⁵

Resorption of the implant material was not obvious in the specimens, and it appears from the studies in dog mandibles⁵ and long bones¹¹ that biodegradation of Interpore 200 is a very slow process. In the dog, biodegradation was clearly detected at 1 year postimplantation. It would be reasonable to assume that any resorption of Interpore 200 in human periodontal tissues may be even slower than in the animal model systems.

The tissue response to metal endosseous implants in rhesus monkeys has been described by Mazzotti et al.²⁶ The connective tissue laid down immediately adjacent to the implant was composed of a layer 30 to 100 μm in width made up of immature collagen fibers rich in

glycosaminoglycans and with other fibrils probably composed of mucopolysaccharide. In the present study collagen fibers were seen running into newly formed bone which had the same appearance as the alveolar bone reported by Nakamura et al.²³ No evidence of an amorphous layer was seen in the scanning electron micrographs. This may indicate that the differences in implant material, animal species, anatomical region and loading forces are important in determining bone response to foreign materials.

Future studies using block sections from human subjects are necessary to fully understand the dynamics involved in the healing of periodontal defects implanted with Interpore 200. However, the present study demonstrates the ability of this implant material to stimulate osteogenesis when it is placed in human periodontal defects. While there was evidence of bone formation in the samples evaluated, comprehensive sampling of a large number of successful cases will be necessary before it will be clear as to the frequency or predictability of bone ingrowth.

ACKNOWLEDGMENT

The authors wish to acknowledge the technical assistance of Ms. Joyce Schumann and Ms. Sarah Beydler.

REFERENCES

- White, R. A., Weber, J. N., and White, E. W.: Replamineform: a new process for preparing porous ceramic metal and polymer prosthetic materials. *Science* **176**: 922, 1972.
- Roy, D. M., and Linnehan, S. K.: Hydroxylapatite formed from coral skeletal carbonate by hydrothermal exchange. *Nature* **247**: 220, 1974.
- Eysel, W., and Roy, D. M.: Topotactic reaction of aragonite to hydroxylapatite. *Z Kristallographic* **141**: 11, 1975.
- Jarcho, M.: Calcium phosphate ceramics as hard tissue prosthetics. *Clin Orthop* **157**: 259, 1981.
- Holmes, R. E.: Bone regeneration within a coralline hydroxylapatite implant. *Plast Reconstr Surg* **63**: 626, 1979.
- Chiroff, R. T., White, E. W., Weber, J. N., and Roy, D. M.: Tissue ingrowth in replamineform implants. *J Biomed Mater Res* **6**: 29, 1975.
- Finn, R. A., Bell, W. H., and Brammer, J. A.: Interpositional grafting with autogenous bone and coralline hydroxylapatite. *J Maxillofac Surg* **8**: 217, 1980.
- Piecuch, J. F., Topazian, R. G., Skoly, S., and Woolfe, S.: Experimental ridge augmentation with porous hydroxylapatite implants. *J Dent Res* **62**: 148, 1983.
- Roser, S. M., Brady, F. A., and McKelvy, B.: Tissue implants of hydroxylapatite replamineform implants in the dog. *J Dent Res* **56**: B172, 1977.
- Holmes, R., Mooney, V., and Bucholz, R.: Regeneration within canine radius defects treated by coralline implants and iliac autografts. *Trans Orthop Res Soc* **6**: 229, 1981.
- Holmes, R. E., and Mooney, V.: Bone regenerated in canine radius defects treated by coralline implants and iliac grafts. *Trans Soc Biomater* **7**: 154, 1984.
- Holmes, R. E., Salyer, K. E., and Hanusiak, W. M.: Bone regeneration in onlay replamineform hydroxylapatite implants. *Trans Soc Biomater* **2**: 180, 1978.
- Mitchell, O. G., Singh, I. J., Klein, I., and Roy, D. M.: Histologic evaluation of porous hydroxylapatite implants in rat bone. *J Dent Res* **55**: B243, 1976.
- Salyer, K., Holmes, R., and Johns, D.: Replamineform porous

hydroxylapatite as bone substitute in craniofacial osseous reconstruction. *J Dent Res* 56: B173, 1977.

15. West, T. L., and Brustein, D. D.: Comparison of replamine-form coral and bone alloplants in dog periodontal pockets. *J Dent Res* 57: 101, 1978.

16. Kenney, E. B., Lekovic, V., Han, T., et al.: The use of a porous hydroxylapatite implant in periodontal defects I. Clinical results after 6 months. *J Periodontol* 56: 82, 1985.

17. Anderson, T. F.: Techniques for the preservation of three dimensional structure in preparing specimens for the electron microscope. *Trans NY Acad Sci* 13: 130, 1951.

18. Ornoy, A., Atkins, J., and Levy, J.: Ultrastructural studies on the origin and structure of matrix vesicles of young rats. *Acta Anat* 106: 450, 1981.

19. Froum, S. J., Kushner, L., Scoop, I. W., and Stahl, S. S.: Human clinical and histological response to durapatite implants in intraosseous lesions. Case reports. *J Periodontol* 53: 719, 1982.

20. Stahl, S. S., Froum, S. J., and Kushner, L.: Healing responses of human intraosseous lesions following the use of debridement grafting and citric acid root treatment. II. Clinical and histologic observations 1 year postsurgery. *J Periodontol* 54: 325, 1983.

21. Moskow, B. S., and Lubarr, A.: Histologic assessment of human periodontal defect after durapatite ceramic implant report of a case. *J Periodontol* 54: 455, 1983.

22. Jones, S. J., and Boyde, A.: Scanning electron microscopy of bone cells in culture. D. H. Copp, and R. V. Talmage (eds), *Proceedings of the Sixth Parathyroid Conference*, pp 97-104. Amsterdam, Excerpta Medica, 1977.

23. Nakamura, Y., Hirashita, A., Kuwabara, Y., and Kawamoto, T.: Scanning electron microscopic observations of the relationship of principal fibers-fibrils and fibrils-osteoblasts in rat periodontium. *J Electron Microsc* 3: 209, 1977.

24. Rovinsky, Y. A., and Slavnaya, I. L.: Spreading of fibroblast-like cells on grooved surfaces. A study by scanning electron microscopy. *Exp Cell Res* 84: 199, 1974.

25. Feren, K., and Reith, A.: Surface topography and other characteristics of nontransformed and carcinogen-transformed C3H 10T1/2 cells in mitosis as revealed by quantitative scanning electron microscopy. *Scan Electron Microsc* 197, 1981.

26. Mazzotti, G., Ruggeri, A., Ottaini, V., and Maraldi, N. M.: Ricerche istochimiche ed ultrastrutturali sul consolidamento dell' impianto endosseo dentario in Macacus Fascicularis. *Minerva Stomatol* 33: 405, 1984.

Send reprint requests to: Dr. E. Barrie Kenney, Section of Periodontics, School of Dentistry, University of California Los Angeles, Los Angeles, CA 90024.

Announcement

THE NORTHEASTERN SOCIETY OF PERIODONTISTS

The Northeastern Society of Periodontists announces its Scientific Program—Spring Meeting.

DATE: Friday, April 11, 1986

TIME: 9:30 AM to 4:00 PM

PLACE: Omni Park Central Hotel,
Seventh Ave. at 56th Street
New York City, NY

TOPIC: Refractory Periodontitis

SPEAKERS: Dr. Russell Nisengard (Immunological Aspects)

Dr. Ann Haffajee (Microbiological Aspects)

Dr. John Prichard (Clinical Aspects)

Dr. Irwin Mandel—Moderator

Dr. Herbert Oshrain—Program Chairman

For further information contact: Irwin W. Scopp, DDS, Secretary-Treasurer, Northeastern Society of Periodontists, Veterans Administration Medical Center, 408 First Ave, New York, NY 10010.